



Optical fabrication and characterisation of SU-8 disk photonic waveguide heterostructure cavities

LUKE P. NUTTALL,¹ FREDERIC S. F. BROSSARD,² STEPHEN A. LENNON,¹ BENJAMIN P. L. REID,¹ JIANG WU,³ JONATHAN GRIFFITHS,⁴ AND ROBERT A. TAYLOR^{1,*}

¹Clarendon Laboratory, Department of Physics, University of Oxford, Oxford, OX1 3PU, UK

²Hitachi Cambridge Laboratory, Hitachi Europe Ltd, Cambridge, CB3 0HE, UK

³Department of Electronic and Electrical Engineering, University College London, Torrington Place, London, WC1E 7JE, UK

⁴Cavendish Laboratory, University of Cambridge, J. J. Thomson Avenue, Cambridge, CB3 0HE, UK

*robert.taylor@physics.ox.ac.uk

Abstract: In order to demonstrate cavity quantum electrodynamics using photonic crystal (PhC) cavities fabricated around self-assembled quantum dots (QDs), reliable spectral and spatial overlap between the cavity mode and the quantum dot is required. We present a method for using photoresist to optically fabricate heterostructure cavities in a PhC waveguide with a combined photolithography and micro-photoluminescence spectroscopy system. The system can identify single QDs with a spatial precision of ± 25 nm, and we confirm the creation of high quality factor cavity modes deterministically placed with the same spatial precision. This method offers a promising route towards bright, on-chip single photon sources for quantum information applications.

Published by The Optical Society under the terms of the [Creative Commons Attribution 4.0 License](https://creativecommons.org/licenses/by/4.0/). Further distribution of this work must maintain attribution to the author(s) and the published article's title, journal citation, and DOI.

OCIS codes: (050.5298) Photonic crystals; (140.3945) Microcavities; (110.5220) Photolithography; (250.5230) Photoluminescence; (230.5590) Quantum-well, -wire and -dot devices.

References and links

1. O. Gazzano and G. S. Solomon, "Toward optical quantum information processing with quantum dots coupled to microstructures," *J. Opt. Soc. Am. B* **33**, C160–C175 (2016).
2. H.-R. Wei and F.-G. Deng, "Scalable quantum computing based on stationary spin qubits in coupled quantum dots inside double-sided optical microcavities," *Sci. Rep.* **4**, 7551 (2014).
3. A. Imamoglu, D. D. Awschalom, G. Burkard, D. P. DiVincenzo, D. Loss, M. Sherwin, and A. Small, "Quantum information processing using quantum dot spins and cavity QED," *Phys. Rev. Lett.* **83**, 4204–4207 (1999).
4. M. Rau, T. Heindel, S. Unsleber, T. Braun, J. Fischer, S. Frick, S. Nauwerth, C. Schneider, G. Vest, S. Reitzenstein, M. Kamp, A. Forchel, S. Höfling, and H. Weinfurter, "Free space quantum key distribution over 500 meters using electrically driven quantum dot single-photon sources - a proof of principle experiment," *New J. Phys.* **16**, 043003 (2014).
5. P. Michler, A. Kiraz, C. Becher, W. V. Schoenfeld, P. M. Petroff, L. Zhang, E. Hu, and A. Imamoglu, "A quantum dot single-photon turnstile device," *Science* **290**, 2282–2285 (2000).
6. M. D. Birowosuto, H. Sumikura, S. Matsuo, H. Taniyama, P. J. van Veldhoven, R. Nötzel, and M. Notomi, "Fast Purcell-enhanced single photon source in 1,550-nm telecom band from a resonant quantum dot-cavity coupling," *Sci. Rep.* **2**, 321 (2012).
7. M. Dušek, O. Haderka, and M. Hendrych, "Generalized beam-splitting attack in quantum cryptography with dim coherent states," *Opt. Commun.* **169**, 103–108 (1999).
8. C. H. Bennett and G. Brassard, "Quantum cryptography: Public key distribution and coin tossing," in *Proceedings of IEEE International Conference on Computers, Systems and Signal Processing*, (IEEE, 1984), pp. 175–179.
9. E. Knill, R. Laflamme, and G. J. Milburn, "A scheme for efficient quantum computation with linear optics," *Nature* **409**, 46–52 (2001).
10. O. Gazzano, M. P. Almeida, A. K. Nowak, S. L. Portalupi, A. Lemaître, I. Sagnes, A. G. White, and P. Senellart, "Entangling quantum-logic gate operated with an ultrabright semiconductor single-photon source," *Phys. Rev. Lett.*

- 110, 250501 (2013).
11. S. Noda, "Seeking the ultimate nanolaser," *Science* **314**, 260–261 (2006).
 12. H. Kim, R. Bose, T. C. Shen, G. S. Solomon, and E. Waks, "A quantum logic gate between a solid-state quantum bit and a photon," *Nat. Photonics* **7**, 373–377 (2013).
 13. C. Simon, M. Afzelius, J. Appel, A. Boyer de la Giroday, S. J. Dewhurst, N. Gisin, C. Y. Hu, F. Jelezko, S. Kröll, J. H. Müller, J. Nunn, E. S. Polzik, J. G. Rarity, H. De Riedmatten, W. Rosenfeld, A. J. Shields, N. Sköld, R. M. Stevenson, R. Thew, I. A. Walmsley, M. C. Weber, H. Weinfurter, J. Wrachtrup, and R. J. Young, "Quantum memories," *Eur. Phys. J. D* **58**, 1–22 (2010).
 14. S. Varoutsis, S. Laurent, P. Kramper, A. Lemaître, I. Sagnes, I. Robert-Philip, and I. Abram, "Restoration of photon indistinguishability in the emission of a semiconductor quantum dot," *Phys. Rev. B* **72**, 041303 (2005).
 15. E. M. Purcell, "Spontaneous emission probabilities at radio frequencies," *Phys. Rev.* **69**, 681 (1946).
 16. D. Englund, I. Fushman, and J. Vuckovic, "General recipe for designing photonic crystal cavities," *Opt. Express* **13**, 5961–5975 (2005).
 17. H.-Y. Ryu, M. Notomi, and Y.-H. Lee, "High-quality-factor and small-mode-volume hexapole modes in photonic-crystal-slab nanocavities," *Appl. Phys. Lett.* **83**, 4294–4296 (2003).
 18. A. Badolato, K. Hennessy, M. Atatüre, J. Dreiser, E. Hu, P. M. Petroff, and A. Imamoglu, "Deterministic coupling of single quantum dots to single nanocavity modes," *Science* **308**, 1158–1161 (2005).
 19. P. B. Joyce, T. J. Krzyzewski, G. R. Bell, and T. S. Jones, "Surface morphology evolution during the overgrowth of large InAs-GaAs quantum dots," *Appl. Phys. Lett.* **79**, 3615–3617 (2001).
 20. K. H. Lee, F. S. F. Brossard, M. Hadjipanayi, X. Xu, F. Waldermann, A. M. Green, D. N. Sharp, A. J. Turberfield, D. A. Williams, and R. A. Taylor, "Towards registered single quantum dot photonic devices," *Nanotechnology* **19**, 455307 (2008).
 21. M. Notomi, "Manipulating light with strongly modulated photonic crystals," *Rep. Prog. Phys.* **73**, 096501 (2010).
 22. E. Kuramochi, M. Notomi, S. Mitsugi, A. Shinya, T. Tanabe, and T. Watanabe, "Ultra-high-Q photonic crystal nanocavities realized by the local width modulation of a line defect," *Appl. Phys. Lett.* **88**, 041112 (2006).
 23. B.-S. Song, S. Noda, T. Asano, and Y. Akahane, "Ultra-high-Q photonic double-heterostructure nanocavity," *Nat. Mater.* **4**, 207–210 (2005).
 24. B.-S. Song, T. Asano, and S. Noda, "Physical origin of the small modal volume of ultra-high-Q photonic double-heterostructure nanocavities," *New J. Phys.* **8**, 209 (2006).
 25. S. Tomljenovic-Hanic, C. M. de Sterke, M. J. Steel, B. J. Eggleton, Y. Tanaka, and S. Noda, "High-Q cavities in multilayer photonic crystal slabs," *Opt. Express* **15**, 17248–17253 (2007).
 26. S. Prorok, A. Petrov, M. Eich, J. Luo, and A. K.-Y. Jen, "Configurable silicon photonic crystal waveguides," *Appl. Phys. Lett.* **103**, 261112 (2013).
 27. S. Gardin, F. Bordas, X. Letartre, C. Seassal, A. Rahmani, R. Bozio, and P. Viktorovitch, "Microlasers based on effective index confined slow light modes in photonic crystal waveguides," *Opt. Express* **16**, 6331–6339 (2008).
 28. M.-K. Seo, J.-H. Kang, M.-K. Kim, B.-H. Ahn, J.-Y. Kim, K.-Y. Jeong, H.-G. Park, and Y.-H. Lee, "Wavelength-scale photonic-crystal laser formed by electron-beam-induced nano-block deposition," *Opt. Express* **17**, 6790–6798 (2009).
 29. K. H. Lee, A. M. Green, R. A. Taylor, D. N. Sharp, J. Scrimgeour, O. M. Roche, J. H. Na, A. F. Jarjour, A. J. Turberfield, F. S. F. Brossard, D. A. Williams, and G. A. D. Briggs, "Registration of single quantum dots using cryogenic laser photolithography," *Appl. Phys. Lett.* **88**, 193106 (2006).
 30. A. F. Oskooi, D. Roundy, M. Ibanescu, P. Bermel, J. D. Joannopoulos, and S. G. Johnson, "MEEP: A flexible free-software package for electromagnetic simulations by the FDTD method," *Comput. Phys. Commun.* **181**, 687–702 (2010).
 31. D. C. Reynolds, K. K. Bajaj, C. W. Litton, G. Peters, P. W. Yu, and J. D. Parsons, "Refractive index, n , and dispersion, $-dn/d\lambda$, of GaAs at 2 K determined from Fabry-Perot cavity oscillations," *J. Appl. Phys.* **61**, 342–345 (1987).
 32. T. C. Sum, A. A. Bettiol, J. A. van Kan, F. Watt, E. Y. B. Pun, and K. K. Tung, "Proton beam writing of low-loss polymer optical waveguides," *Appl. Phys. Lett.* **83**, 1707–1709 (2003).
 33. Y. Tanaka, T. Asano, R. Hatsuta, and S. Noda, "Investigation of point-defect cavity formed in two-dimensional photonic crystal slab with one-sided dielectric cladding," *Appl. Phys. Lett.* **88**, 011112 (2006).
 34. F. Brossard, S. Schirmer, A. Chalcraft, and D. Whittaker, "High Q photonic crystal cavities with tapered air holes," *Proc. SPIE* **7933**, 79331W (2011).
 35. F. S. F. Brossard, X. L. Xu, D. A. Williams, M. Hadjipanayi, M. Hugues, M. Hopkinson, X. Wang, and R. A. Taylor, "Strongly coupled single quantum dot in a photonic crystal waveguide cavity," *Appl. Phys. Lett.* **97**, 111101 (2010).
 36. X. Letartre, C. Seassal, C. Grillet, P. Rojo-Romeo, P. Viktorovitch, M. L. V. d'Yerville, D. Cassagne, and C. Jouanin, "Group velocity and propagation losses measurement in a single-line photonic-crystal waveguide on InP membranes," *Appl. Phys. Lett.* **79**, 2312–2314 (2001).
 37. D. W. Marquardt, "An algorithm for least-squares estimation of nonlinear parameters," *J. Soc. Ind. Appl. Math.* **11**, 431–441 (1963).
-

1. Introduction

Optical cavities coupled to quantum dots (QDs) are of great interest in the field of quantum information processing [1–4]. Coupled cavity-dot systems can function as efficient single photon sources [5, 6] which can be used to mitigate photon number splitting attacks [7] against quantum key distribution protocols [8]. Single photons can also serve as flying qubits for an optical quantum computer [9, 10] and cavity-enhanced spontaneous emission from QDs could enable the creation of thresholdless nanolasers [11]. The strong coupling regime allows for the photon-photon interactions necessary to implement optical quantum logic gates [12] and the strong light-matter interactions required for deterministic quantum memory [13].

When developing single photon sources it is important to minimise the emission lifetime of the QD because this leads to greater photon indistinguishability [14]. For quantum computing applications it is also essential to maximise brightness in order to scale to large computational Hilbert spaces [1]. To achieve both of these goals the ratio of the cavity's quality factor (Q) to its mode volume (V) must be large since it determines the Purcell factor [15, 16]. Additionally, to achieve strong coupling it is necessary for the cavity to have a high Q/\sqrt{V} ratio [16]. Photonic crystal (PhC) cavities can be engineered with high quality factors and very small mode volumes [17], making them ideal for these applications.

In order to achieve coupling between a QD and an optical cavity, the emission from the QD must overlap both spectrally and spatially with the optical mode of the cavity [18]. The standard practice for fabricating dot-coupled PhC cavities uses electron-beam lithography. Epitaxially grown QDs are randomly distributed over the sample and capped by further bulk growth. While uncapped QDs can be easily seen with a scanning electron microscope (SEM), thick capping layers of more than 100 Å obscure the QDs leaving surface deformations of less than 30 Å [19]. Such small changes in surface height cannot be readily detected under SEM, making it very difficult to reliably position cavities around them. Therefore, achieving the necessary spatial and spectral overlap between the cavity mode and QD for on-chip coupling is a matter of luck and the yield for successful fabrication of strongly coupled devices is typically less than 1% [20]. The very low yield renders this method impractical for production of devices containing more than a single dot-cavity structure.

One promising class of PhC cavity designs is modulated mode-gap cavities [21]. These cavities are typically achieved by displacing the holes closest to the waveguide [22] or altering the lattice constant [23] along a small region of the waveguide. A small range of frequencies is allowed to propagate in the heterogeneous region but falls within the photonic stop gap of the rest of the waveguide, thus giving rise to cavity modes with small mode volume [24]. Theoretical studies have also shown that very high Q cavities can be obtained using the same principle by depositing a low refractive index material on top of a PhC waveguide [25]. However, to date there have been very few experimental demonstrations, all based on either electron-beam exposure or deposition techniques [26–28] without the possibility of deterministic coupling to QDs.

In this letter we present a novel method of creating a modulated mode-gap cavity using photolithography. The photolithography system is combined with a micro-photoluminescence (μ PL) spectroscopy system which can locate single QDs to a precision of ± 25 nm using the same approach as Lee *et al.* [29]. This approach opens the road for cavities to be fabricated around QDs to achieve reliable spatial and spectral overlap required for coupling.

2. Cavity design and simulations

This cavity design consists of a PhC membrane waveguide with a small, thin disk of photoresist patterned on top of it, as depicted in Fig. 1. The refractive index of the medium is locally increased by the disk of photoresist, resulting in a small mode volume cavity mode as shown in

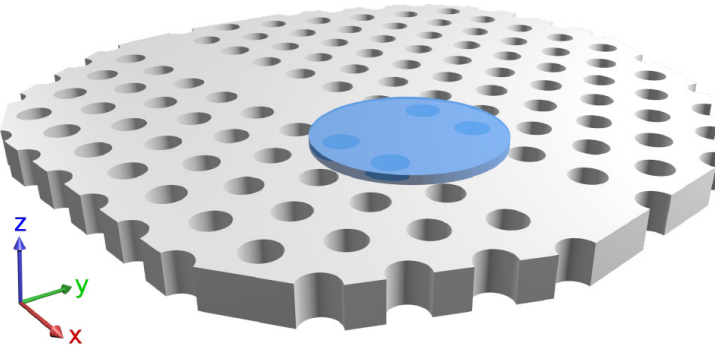


Fig. 1. A 3D rendering showing the structure of a photoresist-on-waveguide cavity. The SU-8 photoresist disk is shown on top of a PhC waveguide. The change in local refractive index due to the presence of the photoresist gives rise to the optical cavity mode.

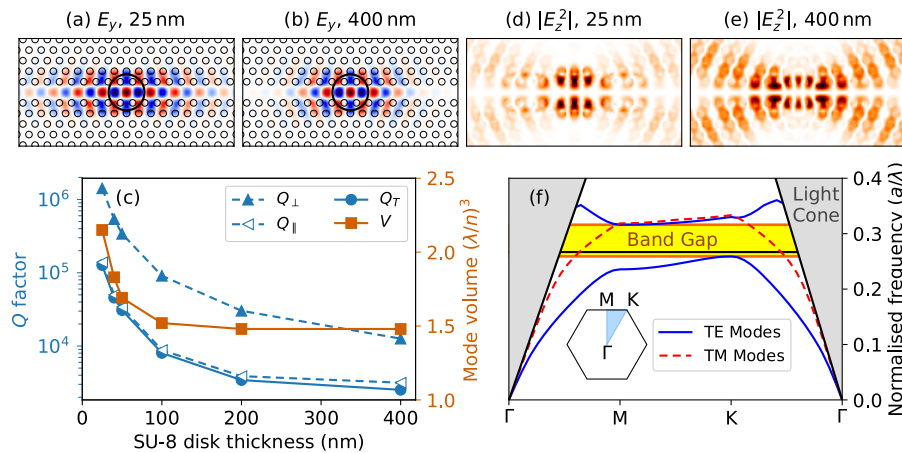


Fig. 2. (a) and (b) Calculated E_y (TE) electric field distributions of the PhC cavity modes created by 25 nm and 400 nm thick SU-8 disks (central black circles) respectively. (c) Calculated Q factor components and mode volume as a function of SU-8 thickness for a 1 μm diameter disk. (d) and (e) Magnitude of E_z^2 (TM) electric field averaged over 4 periods for 25 nm and 400 nm thick SU-8 disks. (f) Band structure showing two TE-like modes (solid lines), the first TM-like mode (dashed line), and the cavity mode frequency (horizontal black line).

Figs. 2(a) and 2(b).

3D electromagnetic field simulations of this device were performed using a freely available software package, MEEP [30], employing a finite-difference time-domain (FDTD) algorithm. The simulated PhC structure had 48 and 24 lattices along the Γ -K and Γ -M directions respectively, a slab thickness of 200 nm, a lattice spacing, a , of 340 nm, and a hole radius of $0.27a$. The refractive indices of GaAs and crosslinked SU-8 were taken to be 3.330 [31] and 1.575 [32] respectively. The diameter of the SU-8 disk was taken to be 1 μm , to match the size of the focused laser spot in the μPL system. The Q factor and mode volume of the cavity mode created by the SU-8 disk were calculated for thicknesses ranging from 25 nm to 400 nm. The total Q factor (Q_T) was decomposed into in-plane (Q_{\parallel}) and out-of-plane (Q_{\perp}) components [16] using flux planes surrounding the PhC. These results, plotted in Fig. 2(c), show that Q_{\perp} is an order of

magnitude larger than Q_{\parallel} for this cavity and thus that Q_T is largely limited by in-plane losses. This is in contrast to a modulated mode-gap cavity with a PhC of same size and same parameters where Q_{\parallel} and Q_{\perp} are nearly equal. Also, we found that increasing the PhC size does not result in an improvement of Q_{\parallel} . We attribute the origin of the lower Q in our device to leaky TM modes generated by the break in the vertical symmetry of the cavity created by the disk [33]. This is corroborated by the increase in the amplitude of the E_z field with increasing thickness as shown in Figs. 2(d) and 2(e) and by the presence of the first TM-like band inside the TE photonic bandgap at the frequency of the cavity mode as shown in Fig. 2(f). However we expect that a PhC with a thinner slab than in the present work would result in much improved Q according to a previous study [34]. We note that the increase in the mode volume for cavities with thin disks is largely compensated by the increase in Q_T , thus such cavities are good candidates for applications requiring strong Purcell enhancement.

3. Device fabrication

The samples studied in this letter consist of GaAs chips with high density self-assembled InGaAs QDs (~ 100 dots/ μm^2) and an AlGaAs sacrificial layer. An array of 2D PhC waveguides was patterned in poly(methyl methacrylate) using a 100 kV VB6 Leica e-beam machine and transferred to the GaAs substrate using reactive ion etching. HF treatment was used to remove the AlGaAs layer beneath the devices, leaving behind suspended PhC membranes containing embedded QDs. The PhC waveguides were designed to support modes at the low-energy tail of the QD distribution. This process is described in more detail by Brossard *et al.* [35].

Before applying the photoresist to the PhC structures, they were first placed inside a continuous flow liquid helium cryostat and cooled down to 4.2 K. Spectroscopy measurements were performed using a μPL system by exciting the QDs above band gap with a He-Ne laser focused through a $100\times$ magnification, 0.5 NA microscope objective to a $\sim 1\ \mu\text{m}$ spot with a power of $6\ \mu\text{W}$ on the sample surface. The emission was collected with the same objective before being directed through a 0.3 m spectrometer onto a 1024 pixel InGaAs array cooled with liquid nitrogen to $-100\ ^\circ\text{C}$. The maximum effective resolution of this spectrometer is 0.05 nm at a wavelength of 1260 nm. The microscope objective was mounted on a piezo-actuated 3-axis translation stage with a $100\ \mu\text{m}$ range on each axis. This was used to scan along the $20\ \mu\text{m}$ length of each waveguide, recording a spectrum every $0.2\ \mu\text{m}$, building up a μPL intensity map. These intensity maps could later be compared to similar maps taken after photolithography in order to demonstrate the creation of cavities.

A photoresist solution was prepared by diluting SU-8 2007 in cyclopentanone. $20\ \mu\text{L}$ of this solution was spincoated onto the samples. The samples were then transferred to a hotplate for a pre-exposure bake at $95\ ^\circ\text{C}$ for 5 minutes to evaporate any remaining solvent. A series of experiments were performed to find the optimal SU-8 concentration and spin speed required to produce a sufficiently thin layer of SU-8 over the PhCs. An atomic force microscope (AFM) was used to measure the thickness of the photoresist layers, whereby the optimal concentration was found to be 1 part SU-8 2007 to 8 parts cyclopentanone by volume and the optimal spin speed was found to be 2800 rpm with an initial angular acceleration of 1000 rpm/s. Due to the small size ($5\times 5\ \text{mm}^2$) of the sample there was still significant variation in thickness between the edges and the centre, where approximately 70 nm thick SU-8 was achievable.

Two different SU-8 exposure protocols were tested using the same optical system as was used for the μPL measurements. Initially a mode locked 800 nm Ti:Sapphire laser with 100 fs pulse duration was used for two-photon exposure of the SU-8 photoresist, as described by Lee *et al.* [20, 29]. A two-photon process was chosen to allow the same laser to be used for μPL excitation and exposure, reducing the risk of alignment errors. However, it was found that the high pulse energy required for two-photon exposure was causing damage to the PhC structure and limiting the Q factor.

To achieve higher Q factors, a 405 nm diode laser was used for resonant exposure of SU-8. For experimental convenience the exposures were performed at room temperature, however the same exposure procedure was performed equally well on a thin SU-8 layer at 4 K. The laser power was $3.4\ \mu\text{W}$ at the focus on the sample and the exposure time was 5 seconds. The laser spot was attenuated by a factor of approximately 10^4 , to avoid exposing the SU-8, and positioned over the centre of the PhC waveguide using the optical image.

After exposing the devices, the sample was developed to remove the unexposed photoresist. First it was baked on a hot plate at $95\ ^\circ\text{C}$ for 5 minutes to allow the photo-acid catalyst (created during the exposure process) to catalyse the crosslinking of the polymer strands. The sample was then immersed in propylene glycol monomethyl ether acetate (PGMEA) and gently agitated for 5 minutes to dissolve the non-crosslinked SU-8. Finally the sample was rinsed with isopropyl alcohol (IPA) and dried with nitrogen gas.

4. Results and discussion

We verified the successful creation of optical cavities by scanning our microscope objective along the length of the waveguide and taking a microphotoluminescence spectrum at each point (spaced by $0.2\ \mu\text{m}$). The data from these hyperspectral maps (taken at 4.2 K) were then compared to equivalent maps before spinning the photoresist.

The “before” and “after” maps for two typical devices are plotted in Fig. 3. It can be clearly seen that in each of the “after” maps, (c) and (f), a cavity mode has been created. Furthermore, these optical modes are spatially confined and located at the centre of the PhC waveguides which matches the location where the SU-8 disks were patterned. These modes are excited indirectly via the photoluminescence from the embedded QDs. The low intensity modes present on each side of the cavity modes are thought to be Fabry-Perot modes created by reflections from the impedance mismatch at the ends of each waveguide [36], and this is evidenced by the presence of these modes in the “before” spectra. Q factors for each cavity were determined by positioning the laser spot over the cavity mode maximum and fitting a Lorentzian function to the resulting spectrum. The measured Q factors ranged from 2.3×10^3 to 7.4×10^3 .

Fig. 4(a) shows a SU-8 disk with diameter $1.2\ \mu\text{m}$ and thickness 230 nm patterned on top of a PhC waveguide with corresponding μPL map shown in Fig. 4(b). The μPL data was collected by raster scanning the objective over the PhC in steps of $0.5\ \mu\text{m}$. It is clear that a PhC cavity has been created at the position of the SU-8 disk.

Additionally, AFM images were taken for all of the fabricated devices to measure the diameter and thickness of the SU-8 disks. A conical frustrum was fitted to each AFM image using the Levenberg-Marquadt algorithm [37] to approximate the disk shape. The SU-8 disks were found to generally be slightly elliptical, as can be seen in Fig. 4, so the quoted diameter is equal to a circle of the same area.

The thickness, diameter and Q factor are plotted in Fig. 5, and it can be seen that thinner disks correlate with smaller disk diameters. One possible explanation is an increase in the total quantity of photoacid catalyst produced in thicker SU-8 layers due to the greater volume of photoresist within the laser spot. An additional explanation could be the variation of light absorption by the SU-8 layer with thickness due to interference effects. We observed significant thickness-dependent interference effects in thin SU-8 films via reflectivity measurements, suggesting that this explanation is plausible.

Thinner photoresist disks correlate with higher Q factors, which is in agreement with the trend predicted by the FDTD simulations in Fig. 2(c). Variations in the position of the disk with respect to the waveguide could explain some of the spread in the Q shown in Fig. 5. The laser spot was viewed through the microscope objective and positioned manually over the waveguide, so the positioning error was on the order of several hundred nanometers. This error can be vastly reduced if we map a single QD, where an accuracy of $\pm 25\ \text{nm}$ is possible [29]. An alternative

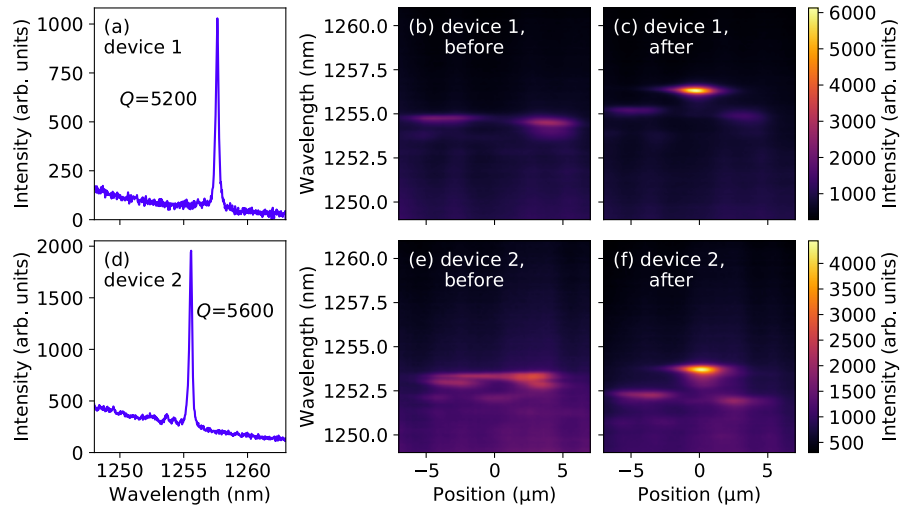


Fig. 3. Plots (a) and (d) show μ PL spectra taken at the centre of the cavity mode on each device. Plots (b), (c), (e), and (f) are 1-dimensional μ PL maps taken before and after fabrication of photoresist disks on top of waveguides. Each map shows the photoluminescence intensity along the waveguide. In (c) and (f) it can be seen that PhC cavity modes have been created.

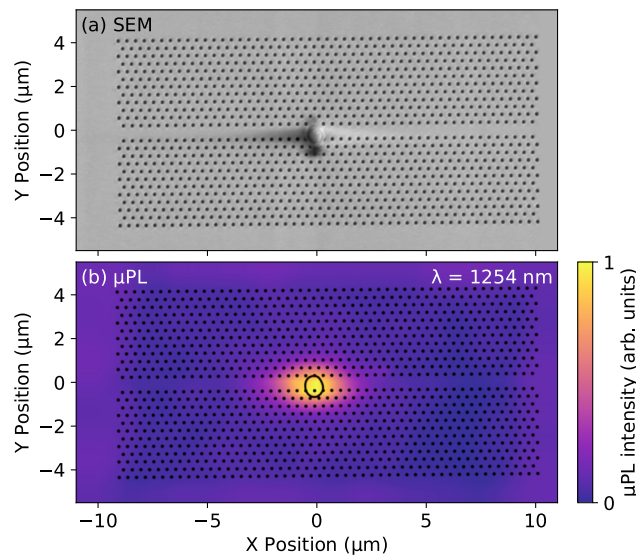


Fig. 4. (a) SEM image of a SU-8 photoresist disk on top of a PhC waveguide. (b) corresponding 2D μ PL map over the same device as (a) at the wavelength of the cavity mode. The black overlay indicates the location of the PhC structure and photoresist disk. This shows that the cavity mode is created at the spatial location of the photoresist disk.

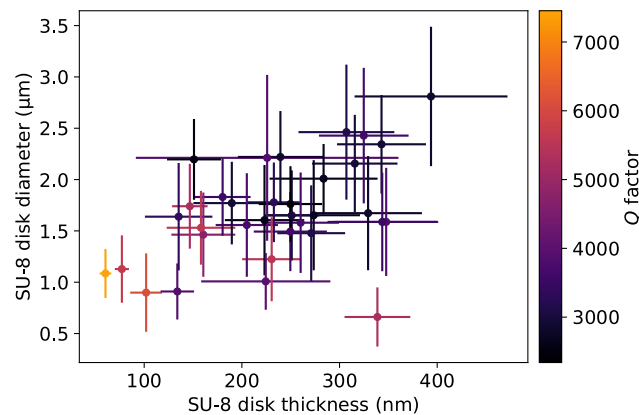


Fig. 5. Q factor of PhC cavities created by photolithography of SU-8 disks as a function of the disk diameter and thickness. Thinner SU-8 clearly correlates with higher Q factors.

approach would be to pattern a strip of SU-8 running perpendicular to the waveguide. The large variation in thickness is due to non-uniformities in the SU-8 layers, most likely caused by differences in position and wettability between PhC structures. The simulations suggest that $Q > 10^4$ could be achieved for sub-50 nm thick SU-8 layers, however more work will be needed to fabricate such a thin layer with any reliability. For layer thicknesses between 50 nm and 200 nm numerical simulations show that the mode wavelength varies by only ~ 2 nm, which allows for fine tuning of the resonance. If a single dot in a low-density sample is to be coupled using this technique, the dot has to be within ± 80 nm of an anti-node in the cavity, which is situated centrally between two holes in the waveguide (see Fig. 2(a)). This can be accomplished, given the spatial accuracy with which the center of the waveguide can be registered, provided the dot is chosen with an emission wavelength slightly to the blue of the cavity mode. Quantum dots can be temperature tuned to the red by ~ 0.8 nm [35], thus allowing coupling to be achieved.

5. Conclusions

In summary, we have developed a method for fabricating photonic microcavities at arbitrary locations along a pre-existing PhC waveguide using all-optical laser lithography. The method involves laser patterning a negative photoresist (SU-8) on top of the PhC waveguide. PhC cavities with Q up to 7000 were achieved. The ability to position and fabricate high Q cavity modes using an optical system capable of locating individual QDs with a spatial precision of ± 25 nm would greatly increase the probability of spatial overlap between QD and cavity modes. Compared to a typical yield of 1 % for strongly coupled QD-cavity devices with e-beam defined cavities, this represents a significant step forward towards reproducible QD-cavity coupling.

Data for the figures can be downloaded at: <https://doi.org/10.5287/bodleian:KZQA7ygmw>

Funding

Engineering and Physical Sciences Research Council (EPSRC) (EP/K014978/1); Hitachi Cambridge Laboratory.